Title	Effect on ^{99}Mo-adsorption/^{99m}Tc-elution properties of alumina with different surface structures
Author(s)	Fujita Yoshitaka, Seki Misaki, Sano Tadafumi, Fujihara Yasuyuki, Kitagawa Tomoya, Matsukura Minoru, Hori Junichi, Suzuki Tatsuya, Tsuchiya Kunihiko
Citation	Journal of Radioanalytical and Nuclear Chemistry,327(3), p.1355-1363
Text Version	Accepted Manuscript
URL	https://jopss.jaea.go.jp/search/servlet/search?5070742
DOI	https://doi.org/10.1007/s10967-021-07616-z
Right	This is a post-peer-review, pre-copyedit version of an article published in Journal of Radioanalytical and Nuclear Chemistry. The final authenticated version is available online at: https://doi.org/10.1007/s10967-021-07616-z

Effect on ^{99}Mo-adsorption/^{99m}Tc-elution Properties of Alumina with Different Surface Structures

Yoshitaka Fujita[1*,4], Misaki Seki[1], Tadafumi Sano[2], Yasuyuki Fujihara[3], Tomoya Kitagawa[5], Minoru Matsukura[5], Junichi Hori[3], Tatsuya Suzuki[4], Kunihiko Tsuchiya[1]

[1] *Department of JMTR, Japan Atomic Energy Agency, 4002 Narita, Oarai, Ibaraki, 311-1393 Japan*

[2] *Atomic Energy Research Institute, Kindai University, 3-4-1 Kowakae, Higashiosaka City, Osaka, 577-8502 Japan*

[3] *Institute for Integrated Radiation and Nuclear Science, Kyoto University, 2 Asashiro-Nishi, Kumatori, Osaka 590-0494 Japan*

[4] *Graduate School of Engineering, Nagaoka University of Technology, 1603-1 Kamitomioka, Nagaoka, Niigata, 940-2188 Japan*

[5] *UNION SHOWA K.K., 1-8-40 Kounan, Minato-ku, Tokyo, 108-0075, Japan*

* fujita.yoshitaka@jaea.go.jp; +81-29-267-1919 (ext. 7042); 0000-0001-9585-4145

Abstract

We prepared three types of Al_2O_3 with different surface structures and investigated ^{99}Mo-adsorption/^{99m}Tc-elution properties using [^{99}Mo]MoO_3 that was irradiated in the Kyoto University Research Reactor. Al_2O_3 adsorbed [^{99}Mo]molybdate ions in solutions at different pH; the lower was the pH, the higher was the Mo-adsorption capacity of Al_2O_3. The ^{99m}Tc-elution properties of molybdate ion adsorbed Al_2O_3 were elucidated by flowing saline. Consequently, it was suggested that ^{99}Mo-adsorption/desorption

properties are affected by the specific surface of Al_2O_3 and ^{99m}Tc-elution properties are affected by the crystal structure of Al_2O_3.

Keywords

Alumina・Mo adsorbent・^{99}Mo/^{99m}Tc generator

Introduction

Medical imaging technology using technetium-99m (^{99m}Tc; $T_{1/2}$ = 6 h) accounts for most nuclear medicine treatments, and more than 30 million tests are conducted worldwide each year. ^{99m}Tc is most commonly used as a radiopharmaceutical. ^{99m}Tc is produced by the decay of ^{99}Mo (^{99}Mo; $T_{1/2}$ = 66 h). Japan is the world's third largest consumer country of ^{99m}Tc after the United States and Europe. However, the domestic demand of Japan relies entirely on imports.

Presently, ^{99}Mo is produced by the fission reaction [(n, f) method] using a uranium target, and the test research reactor constructed 45-55 years ago accounts for 90%-95% of the world's ^{99}Mo supply. In recent years, this supply process has been challenged by the unstable supply of ^{99}Mo/^{99m}Tc because of transportation issues and aging of these reactors [1-3]. Additionally, most uranium targets used in the (n, f) method are made of highly enriched uranium (HEU). The test and research reactors that are planned to be used to produce ^{99}Mo face several issues such as uranium use restriction, nuclear non-proliferation, and nuclear security (i.e., plutonium generation and fission product disposal). Therefore, producing ^{99}Mo by the (n, f) method using HEU is becoming difficult. Hence, there is an ongoing transition around the world from HEU targets to low enriched uranium (LEU) targets. NTP/SAFARI-1 (South Africa) is converting ^{99}Mo production to LEU, and ANSTO Health/OPAL (Australia) is expanding its current LEU-based production [4].

Therefore, a ^{99}Mo production alternative to the (n, f) method, such as ^{99}Mo production by the activation method [(n, γ) method: (n, γ)^{99}Mo] and ^{99}Mo production by the

photonuclear reaction [(γ, n) method: (γ, n)^{99}Mo] [5, 6], is attracting attention. However, because the amount of ^{99}Mo produced by the (γ, n) method is small, irradiating enriched ^{100}Mo is necessary to obtain a sufficient amount of ^{99}Mo produced, which is costly.

Because (n, γ)^{99}Mo can produce a sufficient amount of ^{99}Mo even if natural Mo is used, the cost of raw materials is low. However, because the specific activity of ^{99}Mo produced by this method is lower than that of the (n, f) method, developing Mo adsorbents with high adsorption capacity for the practical application of (n, γ)^{99}Mo is essential. Alumina (Al_2O_3) is commonly used as a Mo adsorbent for generators. Research is also carried out using other materials with good Mo-adsorption properties [7-9]. However, according to Japanese radiopharmaceutical standards, generators using new materials require a long time to obtain approval. Therefore, the development of Al_2O_3 with a high Mo-adsorption capacity is necessary for the early practical use of generators using (n, γ)^{99}Mo. Although Al_2O_3 with high Mo-adsorption capacity has been developed and reported so far, the factors that determine its Mo-adsorption capacity have not been discussed [10-13].

In this study, we focused on three types of Al_2O_3 specimens with different initial materials and evaluated ^{99}Mo-adsorption/^{99m}Tc-elution properties of Al_2O_3 specimens using [^{99}Mo]MoO_3 irradiated at the Kyoto University Research Reactor (KUR). From the obtained results, the effects of the specific surface and crystal structure of each Al_2O_3 specimen on the ^{99}Mo-adsorption/^{99m}Tc-elution properties were investigated.

Experimental

Materials of Al_2O_3 specimens

The raw material of alumina used is aluminum hydroxide, and it is known that alumina produced from aluminum hydroxide has different crystal structures (e.g., gibbsite, p-boehmite, and bayerite) depending on the raw material and sintering temperature [15]. In a previous study [14], we investigated the Mo-adsorption properties of Al_2O_3 specimens prepared from aluminum hydroxide with different crystal structures. To produce Al_2O_3 specimens, 5 wt.% of alumina sol and water were added to each aluminum hydroxide powder, and extrusion molding was conducted. Then, the molded body was dried at

200 °C-300 °C for 1 h, pulverized, and classified with a 50-to-100-mesh sieve (opening: 150-300 μm). Then, it was sintered at 300 °C-1000 °C (interval of 100 °C) for 1 h. It was clarified that Mo adsorption capacities of Al_2O_3 specimens were affected by specific surface area and crystal structure.

Among the Al_2O_3 specimens produced from each aluminum hydroxide, the Al_2O_3 specimens sintered at 300 °C had the highest Mo adsorption capacity; therefore, these specimens were used for further experiments. Here, Al_2O_3 specimens of different crystal structures (e.g., gibbsite, p-boehmite, and bayerite) were referred to as G-Al_2O_3, p-Al_2O_3, and B-Al_2O_3, respectively. Additionally, commercial medical alumina (M-Al_2O_3) was also prepared as a comparative specimen. The basic properties of each Al_2O_3 specimen (that was sintered at 300 ℃) used in the experiment are shown in Table 1.

Table 1 Basic properties of Al_2O_3 specimens

Specimens	Crystal structure	Specific surface (m^2/g)	Particle size (D_{50}) (μm)
G-Al_2O_3	χ-Al_2O_3 + Boehmite	311	283
p-Al_2O_3	p-Boehmite	270	285
B-Al_2O_3	η-Al_2O_3 + Boehmite	417	238
M-Al_2O_3	χ-Al_2O_3 + γ-Al_2O_3	116	103

Neutron Irradiation of MoO_3 specimens

MoO_3 pellets were made from MoO_3 powder produced by TAIYO KOKO CO., LTD. The chemical composition of MoO_3 powder used is shown in Table 2. The MoO_3 powder was mixed with ethanol containing 2 wt.% camphor, molded into pellets by uniaxial pressing, and sintered at 650 °C. Then, after MoO_3 pellets were sufficiently dried, MoO_3 pellets were roughly crushed, and approximately 1.5 g of MoO_3 pieces was used for the neutron irradiation test. When preparing MoO_3 specimens, impurities were prevented from being mixed into the specimens as much as possible. After enclosing MoO_3 specimens in a polyethylene bag, they were enclosed in special polyethylene capsules for the irradiation test.

Table 2 Chemical composition of the MoO_3 powder

Items	Values (%)
loss on ignition	0.08
Na	0.0005
K	0
MgO	0.0001
CaO	0.0001
W	0.002
Fe	0.0001
Cu	0.0003
Al_2O_3	0.001
SiO_2	0.001
Pb	0.001
PO_4	0.0005
S	0.001

MoO_3 specimens were irradiated at 5 MW for 20 min using the irradiation hole of the pneumatic transport tube Pn-2 (thermal neutron flux: 2.8×10^{17} n/m^2/s) of the Kyoto University Research Reactor (KUR). The irradiation conditions are shown in Table 3. After cooling the [^{99}Mo]MoO_3 specimens for 4 d, they were removed from special polyethylene capsules and used to test the ^{99}Mo-adsorption/^{99m}Tc-elution property in the draft chamber of the KUR Hot Lab.

Table 3 Irradiation conditions of MoO_3 pellet pieces in Pn-2

Items	Values
Thermal power	5 MW
Thermal neutron flux	2.8×10^{17} n/m^2/s
Epithermal neutron flux	1.1×10^{16} n/m^2/s
Fast neutron flux	6.0×10^{16} n/m^2/s
Irradiation time	20 min

^{99}Mo-adsorption/^{99m}Tc-elution property test

^{99}Mo-adsorption/^{99m}Tc-elution property tests were conducted using two types of experiments. The first type is a pH-dependent adsorption test used to examine the Mo-adsorption capacity of Al_2O_3 specimens depending on the pH of an aqueous solution of sodium [^{99}Mo]molybdate (Mo solution). The second type is a ^{99m}Tc-elution properties test conducted by flowing saline into Mo-adsorbed Al_2O_3 specimens. All experiments were conducted at room temperature because previous studies showed that Mo-adsorption capacities were not temperature dependent. Approximately 1.5 g of irradiated MoO_3 specimens was dissolved in 3.75 mL of a 6 mol/L-NaOH aqueous solution; then, water was added to adjust to the concentration to 10 mg-Mo/mL and obtain the desired pH. Using the abovementioned procedure, 100 mL of [^{99}Mo]Mo solution was prepared.

In the tests, liquid measurement specimens were prepared by depositing 100 μL of the solution on a Φ10 mm paper disk and encapsulating it in a polyethylene bag. For the pH-dependent adsorption test, the measurement specimens of Al_2O_3 were prepared by filtering the Al_2O_3 specimen after Mo-adsorption with a Φ25 mm filter paper and encapsulating it in a polyethylene bag. The activities were measured using a γ-ray spectrometer made by Mirion Technologies (Canberra) KK. In the measurement, the distance between the detector and measurement specimens was adjusted so that the dead time was 5 % or less. After the measurement, the Mo-adsorption capacity (mg-Mo/g) was calculated based on the ^{99}Mo specific activity at the adsorption start time. The errors by the activity measurement are smaller than those by the chemical operation and can be ignored; thus, they are not considered.

pH-dependent adsorption test

The test procedure for the pH-dependent adsorption test is shown in Fig. 1. From 100 mL of the [^{99}Mo]Mo solution adjusted to pH 7, 15 mL was removed and added to a vial. The separated [^{99}Mo]Mo solution was adjusted to pH 2–7 (pH 1 interval) by adding 2 mol/L-HCl. A total of 3 mL of the prepared [^{99}Mo]Mo solution was added to a microtube containing 0.1 g of each Al_2O_3 specimen and immersed for 3 h to adsorb [^{99}Mo]Mo. After the immersion, the [^{99}Mo]Mo solution and Al_2O_3 specimen were

separated by vacuum filtration, and the Al_2O_3 specimen was washed with 30 mL of water. Then, the activity of ^{99}Mo adsorbed on the Al_2O_3 specimen was measured.

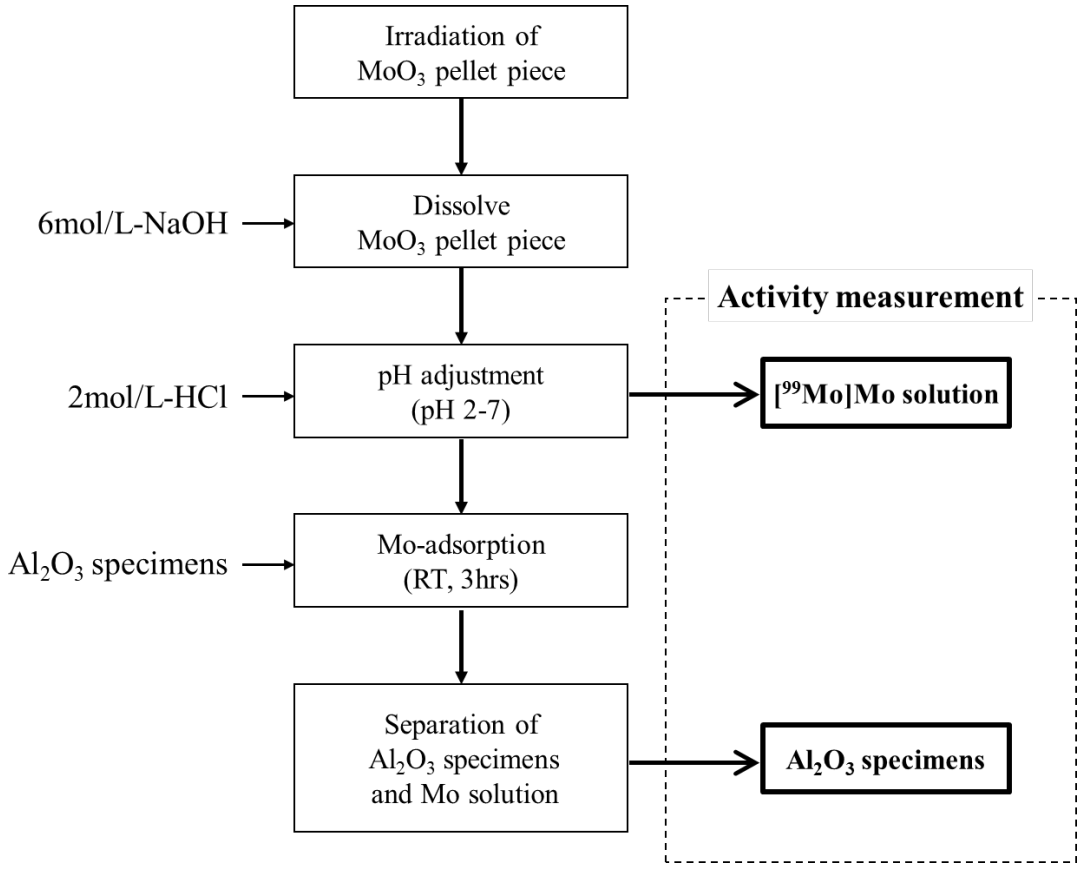

Fig. 1 pH-dependent adsorption test procedure

^{99m}Tc-elution properties test

The test procedure for the ^{99m}Tc-elution properties test is shown in Fig. 2. A total of 30 mL was removed from 100 mL of the [^{99}Mo]Mo solution into a vial containing 1 g of each Al_2O_3 specimen. After immersing for 3 h, the Al_2O_3 specimens and the supernatant were separated. The Mo adsorbed Al_2O_3 specimens are washed with 20 mL of water. Then, the activity of the solution containing the supernatant and the wash solution was measured. The washed Al_2O_3 specimen was packed in a polypropylene column and further washed with 50 mL of water. The column packed with each Al_2O_3 specimen was washed with 50 mL of saline to remove ^{99m}Tc and ^{99}Tc. After 24 h, the column was milked with 1.5 mL of saline six times and 10 mL once for a total of 19 mL to examine

the elution properties of ^{99m}Tc. The activity of ^{99}Mo and ^{99m}Tc in the obtained an aqueous solution of sodium [^{99m}Tc]pertechnetate (^{99m}Tc solution) was measured. The Mo-adsorption capacity of each Al_2O_3 specimen was calculated from the value obtained by subtracting the Mo content in the supernatant and the wash solution from the Mo content in the solution before immersion.

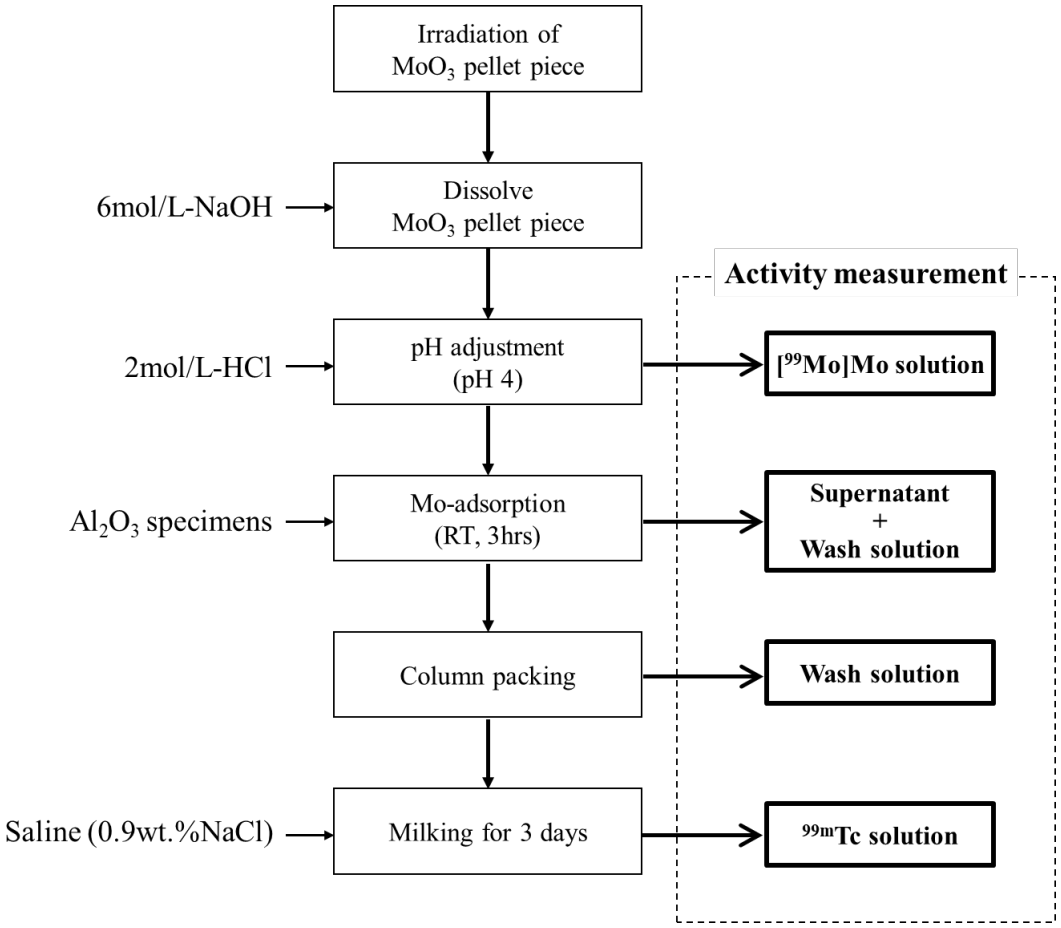

Fig. 2 ^{99m}Tc-elution properties test procedure

Results and discussion

Irradiation properties

An example of the γ-ray spectrum measured to calculate the Mo-adsorption capacity is shown in Fig. S1. This is the γ-ray spectrum of the Mo solution used in the ^{99m}Tc-elution properties test of B-Al_2O_3 and M-Al_2O_3. The activity of ^{99}Mo was calculated by

the Covell method from the energy peak of 739.469 keV specified for the radiopharmaceutical standard. After irradiation, ^{99}Mo and ^{99m}Tc already reached transient equilibrium by cooling for more than 4 d. The peaks of both ^{99}Mo and ^{99m}Tc are clearly shown in Fig. S1. Additionally, a peak of ^{92m}Nb (934.46 keV) generated by the (n, p) reaction from ^{92}Mo was also confirmed because a MoO_3 powder with natural abundance was used in this test.

The ^{99}Mo specific activities in the [^{99}Mo]Mo solution approximately 100 h after the irradiation are shown in Table 4. The values were calculated using the Pn-2 nominal thermal neutron flux of KUR (2.8×10^{17} n/m^2/s) and the capture cross section of ^{98}Mo for thermal neutrons (0.13 barn) [16]; the producing amount of ^{99}Mo immediately after neutron irradiation for 20 min was obtained. The activity of ^{99}Mo after 100 h was calculated from the obtained amount by attenuation correction. Thus, the ratio between calculated and experimental values (C/E) was 0.45-0.62, and the experimental value was approximately twice as high as the calculated value. It is assumed that this increase in ^{99}Mo production is due to the contribution of ^{99}Mo production in the region of epithermal neutrons and fast neutrons [17].

Table 4 Activities of ^{99}Mo in the sodium molybdate solution after approximately 100 h from irradiation completion (1: for G-Al_2O_3 and p-Al_2O_3, 2: for B-Al_2O_3 and M-Al_2O_3)

	pH-dependent adsorption test		**^{99m}Tc-elution properties test**	
	1	**2**	**1**	**2**
Calculation values (MBq/g-Mo)	6.81	6.85	6.83	6.81
Experimental values (MBq/g-Mo)	11.02	15.33	14.59	14.88
C/E	0.62	0.45	0.47	0.46

pH-dependent adsorption test

The Mo-adsorption capacities of each Al_2O_3 specimen depending on the pH of the [^{99}Mo]Mo solution are shown in Fig. 3. Mo-adsorption capacities (mg-Mo/g) were calculated using ^{99}Mo specific activities shown in Table 4. For all Al_2O_3 specimens, it was determined that the higher was the acid concentration of the Mo solution, the higher was the Mo-adsorption capacity. The Mo-adsorption capacities of the developed three types of Al_2O_3 specimens were more than double that of M-Al_2O_3. Specifically, B-Al_2O_3, which had the largest specific surface area, had a slightly superior Mo-adsorption capacity compared with those of the other two specimens.

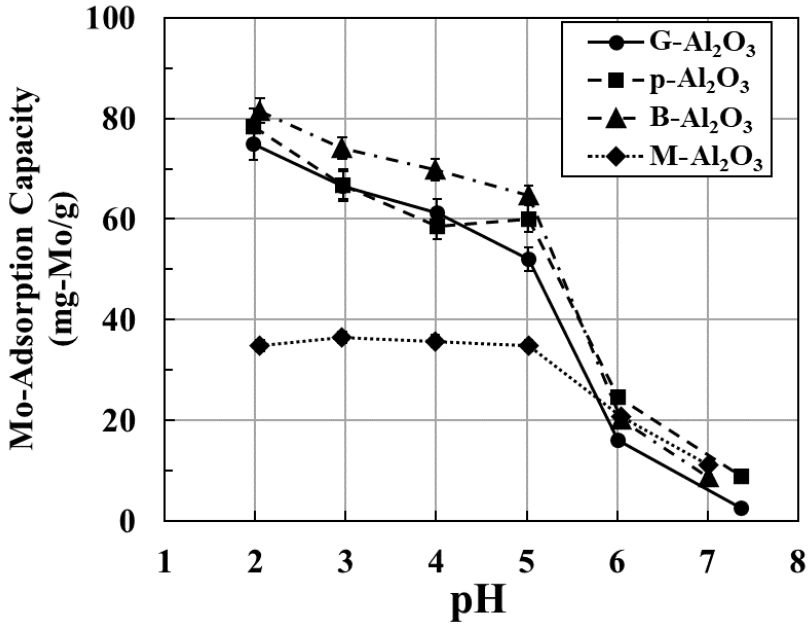

Fig. 3 Mo-adsorption capacities depending on the pH of the Mo solution

It is known that Al_2O_3 exhibits both anion and cation exchange properties. Al_2O_3 hydrates by immersion in an aqueous solution; then, it is converted into an anion exchanger by immersion in an acidic solution [18]. This causes an exchange of surface hydroxyl groups on Al_2O_3 with the anions in solution. Because polyvalent anions are more easily adsorbed on Al_2O_3 than monovalent anions, it is expected that molybdic acid MoO_4^{2-} is preferentially adsorbed on alumina compared with Cl^- of hydrochloric acid. Mo adsorbs on Al_2O_3 by the reaction of Eq. (1) or Eq. (2) near the surface of Al_2O_3 [19]. This reaction causes an increase in the OH^- concentration on the surface of Al_2O_3, which results in a local increase in pH.

$$Al–OH + MoO_4^{2–} \rightarrow Al–OMoO_3^{–} + OH^{–} \quad (1)$$

$$\begin{array}{l} Al–OH \\ \\ \\ Al–OH \end{array} + MoO_4^{2–} \rightarrow \begin{array}{l} Al–O \\ \quad \diagdown \\ \qquad MoO_2 + 2OH^{–} \\ \quad \diagup \\ Al–O \end{array} \quad (2)$$

However, in a solution containing Mo(VI) ions, when the Mo concentration is high ($> 10^{–3}$ M) and the acid concentration increases, it is reported that Mo(VI) ions are polyionized [20, 21]. Therefore, in the test, it is assumed that large quantities of Mo(VI) species (e.g., $Mo_8O_{26}^{4–}$ or $Mo_7O_{24}^{6–}$) exist in the Mo solution used in the acid concentration range of pH 2-5. However, because high Mo-adsorption capacities are obtained at these acid concentrations, Mo(VI) species should be abundant as $MoO_4^{2–}$ on the surface of Al_2O_3. In the literature [22], it has been reported that the equilibrium [as in Eq. (3)] holds in the ammonium heptamolybdate solution.

$$Mo_7O_2^{4-} + 4H_2O \rightleftharpoons 7MoO_4^{2-} + 8H^{+} \quad (3)$$

In Eq. (3), the reaction proceeds to the right with an increase in pH. In the vicinity of the Al_2O_3 surface, the polyanion is decomposed because pH increases because of the adsorption reaction of Eq. (2). Therefore, it is considered that the rightward reaction in Eq. (3) occurs even in the Mo solution containing large quantities of polyanions, and the molybdate ion is adsorbed on Al_2O_3 as $MoO_4^{2–}$.

The comparison of the pH of the [^{99}Mo]Mo solution before Mo-adsorption and the supernatant/washing mixture after Mo-adsorption is shown in Table 5. At pH 2-4, the pH of all Al_2O_3 specimen's mixed solution after Mo-adsorption tended to be more basic than the pH of the [^{99}Mo]Mo solution before Mo-adsorption. However, at pH 5 and above, the pH of all Al_2O_3 specimen's mixed solution after Mo-adsorption tended to be slightly acidic compared with the pH of the [^{99}Mo]Mo solution before Mo-adsorption. Here, because the Mo-adsorption capacity similar to that at pH 4 was obtained at pH 5, it is expected that the $OH^{–}$ concentration increases with Mo-adsorption. Hence, it is speculated that the Mo solution, which became almost neutral, released H^{+} according to the rightward reaction of Eq. (3) and thus became slightly acidic. At pH 6 and pH 7,

231 because almost no Mo-adsorption was observed, it is assumed that the pH of the mixed
232 solution was affected by purified water used for washing. Generally, purified water
233 absorbs CO_2 from the air and becomes mildly acidic. In the experiment, this possibility is
234 high because 30 mL of purified water was added to 3 mL of the supernatant.

235 **Table 5** pH of the Mo solution before Mo-adsorption and supernatant/washing mixture
236 after Mo-adsorption

		Mo solution before adsorption	Supernatant + Wash solution
G-Al_2O_3	**2**	1.98	3.52
	3	2.97	4.28
	4	4.01	4.55
	5	5.02	4.82
	6	6.01	5.82
	7	7.38	7.11
p-Al_2O_3	**2**	1.98	3.41
	3	2.97	4.20
	4	4.01	4.49
	5	5.02	4.79
	6	6.01	5.83
	7	7.38	6.90
B-Al_2O_3	**2**	2.05	3.77
	3	2.96	4.31
	4	3.99	4.55
	5	5.02	4.81
	6	6.04	5.92
	7	7.01	7.10
M-Al_2O_3	**2**	2.05	2.99
	3	2.96	3.58
	4	3.99	4.18
	5	5.02	4.61

6	6.04	5.73
7	7.01	6.65

When comparing the pH changes of the four Al_2O_3 specimens before and after Mo-adsorption, the pH of the mixed solution of M-Al_2O_3 after Mo-adsorption was more acidic than that of other Al_2O_3 specimens. This occurs because M-Al_2O_3 was used as a nominally acidic alumina; because it was initially treated with an acid, some hydroxyl groups on the Al_2O_3 surface had already been replaced with Cl^- or NO_3^-. Thus, it can be inferred that the mixed solution of M-Al_2O_3 was not more biased toward the basicity than the solution of other Al_2O_3 specimens in the ion exchange reaction with MoO_4^{2-}. From the abovementioned results, to obtain a more concentrated ^{99m}Tc solution as a ^{99}Mo/^{99m}Tc generator, it is desirable to adsorb Mo on Al_2O_3 using a [^{99}Mo]Mo solution with a high acid concentration. However, when the Mo solution has a high acid concentration, molybdic acid precipitates. Therefore, it was concluded that the Mo solution of pH 4 was an appropriate adsorption condition because this acid concentration did not cause precipitation of molybdic acid while increasing the Mo-adsorption capacity.

^{99}Mo-adsorption/^{99m}Tc-elution properties of Al_2O_3 specimens

Evaluation of ^{99}Mo-adsorption properties

The results of the Mo-adsorption properties test using a [^{99}Mo]Mo solution are shown in Table 6. The Mo-adsorption capacities (mg-Mo/g-Al_2O_3) were calculated from the ^{99}Mo-adsorption capacities (mg-^{99}Mo/g-Al_2O_3) using ^{99}Mo specific activities shown in Table 4. B-Al_2O_3 had the highest Mo-adsorption capacity and had twice the capacity of M-Al_2O_3. Both G-Al_2O_3 and p-Al_2O_3 have similar adsorption capacities, and both have higher Mo-adsorption capacities than M-Al_2O_3. The specific surface of B-Al_2O_3 is the highest, followed by G-Al_2O_3 and p-Al_2O_3 having the same specific surface and M-Al_2O_3 having the lowest specific surface. Therefore, it was clarified that the Mo-adsorption capacity of Al_2O_3 largely depends on the specific surface.

Table 6 [^{99}Mo]Mo-adsorption capacities per 1 g of each Al_2O_3 specimen

Adsorption capacity	Specimens			
	G-Al_2O_3	**p-Al_2O_3**	**B-Al_2O_3**	**M-Al_2O_3**
MBq-^{99}Mo/g-Al_2O_3	0.91	0.88	1.17	0.59
mg-Mo/g-Al_2O_3	58.4	56.4	74.1	37.2

Evaluation of ^{99m}Tc-elution properties

An example of the γ-ray spectrum, which is used to calculate the ^{99m}Tc-elution rate, is shown in Fig. S2. The abovementioned spectrum is the γ-ray spectrum of the first milking solution of B-Al_2O_3 on day 1. The activities of ^{99m}Tc were calculated by the Covell method from the energy peak at 140.509 keV in the radiopharmaceutical standard. It is confirmed in Fig. S2 that ^{99}Mo is contained in the milked ^{99m}Tc solution. Because the peak of ^{92m}Nb (934.46 keV) contained in the [^{99}Mo]Mo solution shown in Fig. S1 is not observed in Fig. S2, it was confirmed that ^{92m}Nb was not mixed in the ^{99m}Tc solution.

^{99}Mo adsorbed on alumina disintegrated to ^{99m}Tc, and saline was flown every 24 h for milking for 3 d. The elution properties of ^{99m}Tc from each Al_2O_3 specimen are shown in Fig. 4. In the milking on day 1, the elution properties of p-Al_2O_3 and B-Al_2O_3 were excellent, and almost the entire amount of ^{99m}Tc could be eluted by approximately 10 mL of milking. During the milking after day 2, besides the abovementioned two Al_2O_3 specimens, M-Al_2O_3 showed an excellent ^{99m}Tc-elution rate of 100 %. However, the elution rate of G-Al_2O_3 was only approximately 70 % on all 3 d. Because these elution properties do not correlate with the specific surface area, the crystal structure of Al_2O_3 and the surface condition of Al_2O_3 (e.g., pore size) may have an effect. G-Al_2O_3 and M-Al_2O_3 with a relatively low ^{99m}Tc-elution rate contain the crystal structure of χ-Al_2O_3 in common. Therefore, χ-Al_2O_3 is expected to be a crystal structure which is difficult to elute ^{99m}Tc. On the other hand, the crystal structures of boehmite, p-boehmite and η-Al_2O_3 are considered to have similar ^{99m}Tc-elution properties.

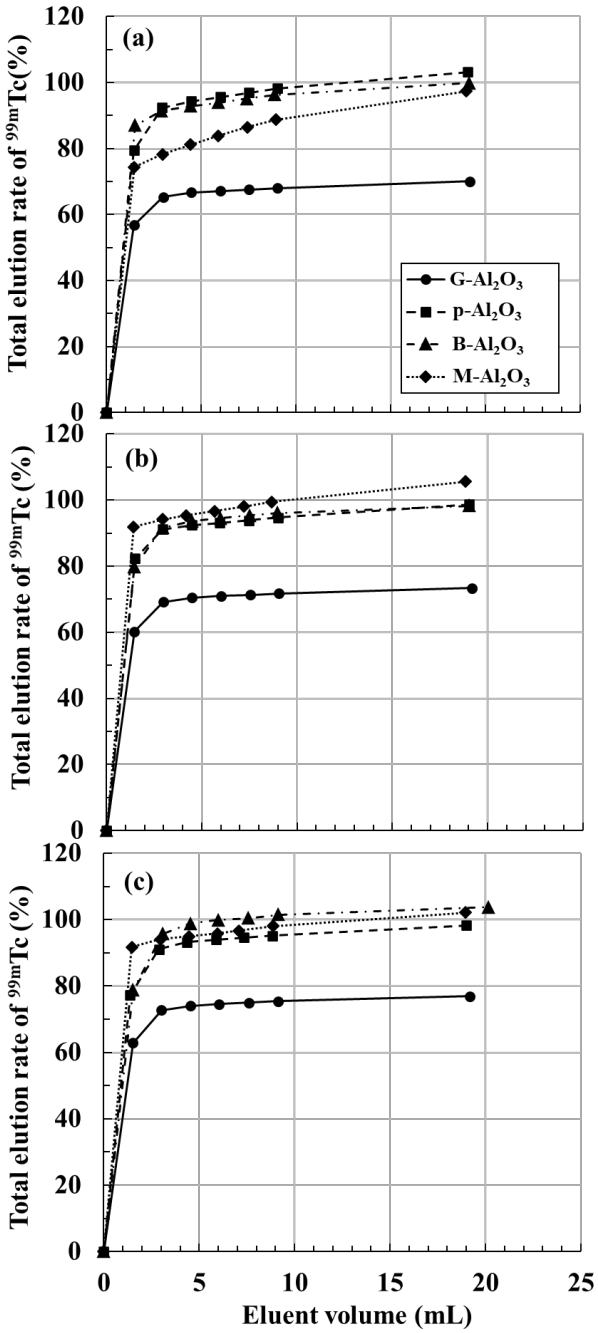

Fig. 4 ^{99m}Tc-elution properties of each Al_2O specimen, (a) Day 1, (b) Day 2, (c) Day 3

The decay of [^{99}Mo]molybdate on the alumina column occurs according to Eq. (4).

$$^{99}MoO_4^{2-} \rightarrow \beta' + {}^{99m}TcO_4^- \quad (4)$$

Technetium is a homologous element to rhenium, and pertechnetate and perrhenate behave similarly on Al_2O_3. Rhenium supported on Al_2O_3 has a small interaction because it exists as tetrahedral ReO_4^- and experiences dynamic strain by Al_2O_3 or surface OH groups [23]. Therefore, it is assumed that tetrahedral TcO_4^- on Al_2O_3 also has a weak interaction and can be easily replaced [24]. Specifically, because the interaction between Cl^- ions contained in saline (0.9 wt.% NaCl) and Al_2O_3 is relatively strong [18], it is assumed that tetrahedral TcO_4^- can be easily replaced.

Quality evaluation of the ^{99m}Tc solution

The pH of the ^{99m}Tc solution milked from each Al_2O_3 specimen is shown in Fig. 5. Here, the pH of the ^{99m}Tc solution is a measured value of a total of 9 mL obtained by mixing the milked solutions of the first to sixth times. According to Japanese radiopharmaceutical standards, the pH range of the ^{99m}Tc solution is specified as pH 4.5-7.0. G-Al_2O_3 and B-Al_2O_3 satisfy the standard value of pH. However, the pH of p-Al_2O_3 is close to the lower limit, and the pH of M-Al_2O_3 deviates from the standard value. In the radiopharmaceutical standard, the amount of ^{99}Mo-desorbed into a ^{99m}Tc solution is determined using the ^{99}Mo/^{99m}Tc ratio as an index. The standard value is ^{99}Mo/^{99m}Tc < 0.015 %. The ^{99}Mo/^{99m}Tc ratio during milking for 3 d in this test is shown in Fig. 6. The ^{99}Mo/^{99m}Tc ratio was highest in the solution of M-Al_2O_3, followed by that of p-Al_2O_3. Those of G-Al_2O_3 and B-Al_2O_3 were comparable and less than half of the value of the previous two solutions. It was already reported that M-Al_2O_3 has the smallest specific surface and almost no surface irregularities [14]. Therefore, it is considered that the [^{99}Mo]molybdate ion adsorbed on M-Al_2O_3 under this condition was desorbed by the flow of saline. On the other hand, since B-Al_2O_3 has a large specific surface, many irregularities and pores, it is expected that [^{99}Mo]molybdate ions are strongly retained and be difficult to be desorbed.

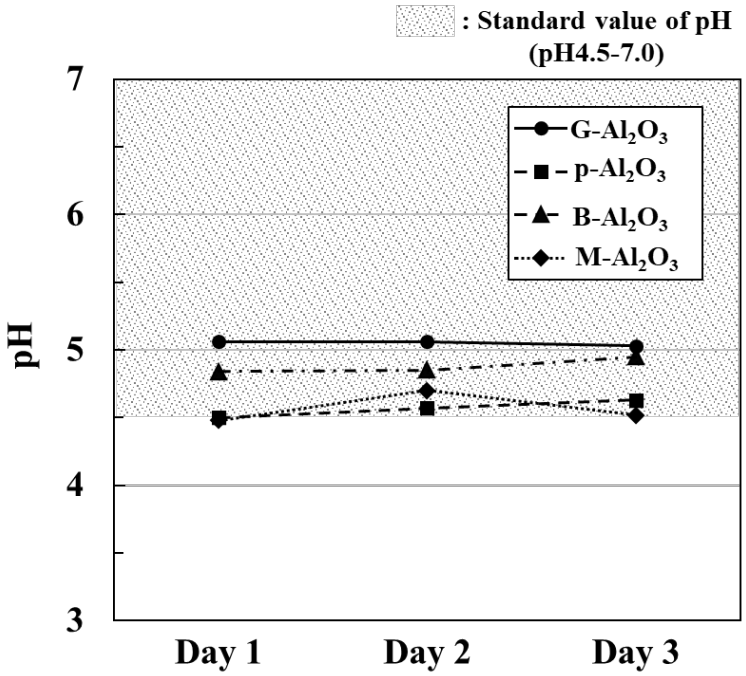

Fig. 5 The pH of the ^{99m}Tc solution on each Al_2O_3 specimen

The amount of Mo desorbed correlates with the pH results of the ^{99m}Tc solution described above. Specifically, the larger is the amount of Mo desorbed in the ^{99m}Tc solution, the lower is the pH of the solution. It is assumed that Mo separated from the Al_2O_3 column is desorbed as $Mo_7O_{24}^{6-}$ in a small amount of slightly acidic saline added by milking. Here, it is reported that when the Mo concentration in the Mo solution is low ($< 10^{-3}$), molybdate ions exist as MoO_4^{2-} [20]. Therefore, Mo adsorbed on the Al_2O_3 is desorbed as $Mo_7O_{24}^{6-}$, and the reaction shifts to the right side according to the equilibrium in Eq. (1) in the ^{99m}Tc solution. Thus, it is assumed that $Mo_7O_{24}^{6-}$ dissociates into MoO_4^{2-}, and the pH of the solution becomes acidic.

To meet the radiopharmaceutical standards for both the ^{99}Mo/^{99m}Tc ratio and pH, it is essential to prevent ^{99}Mo-desorption from Al_2O_3. In Fig. 6, it is shown that although an increase in the ^{99}Mo/^{99m}Tc ratio decreases with an increase in the amount of eluent, it increases almost linearly under the test conditions up to 19 mL of milking. In the static adsorption method used in this test, during which Al_2O_3 is immersed in the Mo solution, molybdate ions are uniformly adsorbed on the entire Al_2O_3. Because molybdate ions on Al_2O_3 are adsorbed by physical adsorption, which has a relatively weak adsorptive power,

it is assumed that desorption of molybdate ions at the bottom of the column is unavoidable when flowing saline.

Therefore, to use these Al_2O_3 specimens in a generator, reducing the amount of desorbed Mo is necessary.

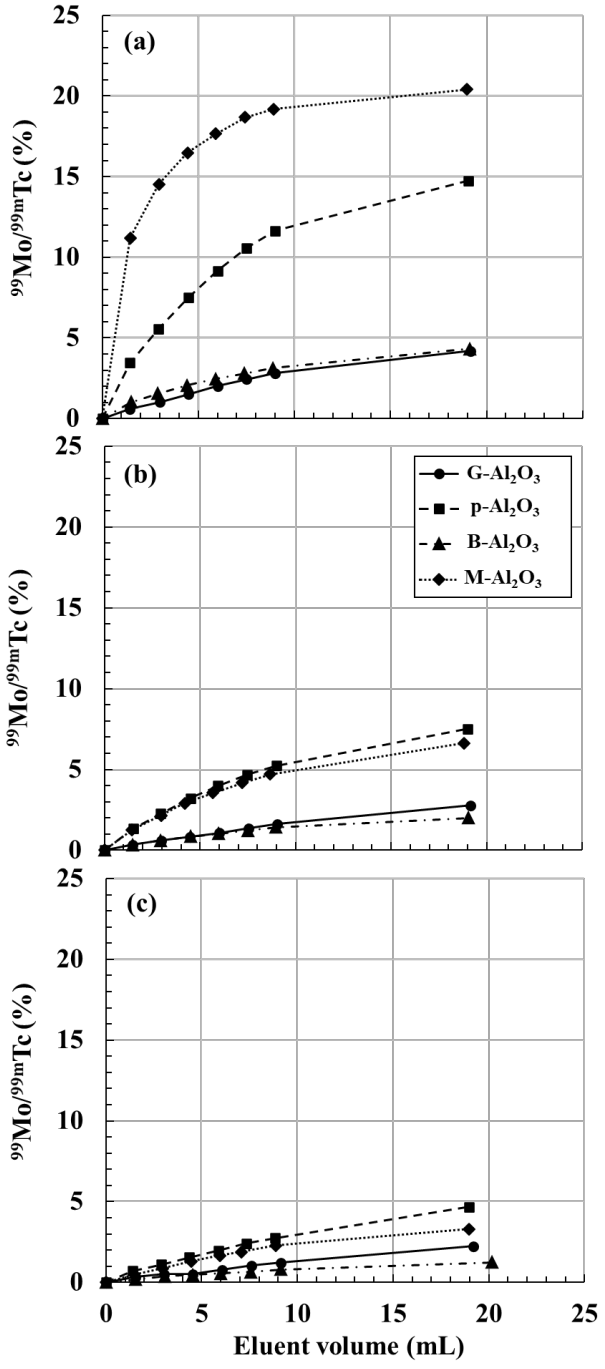

Fig. 6 ^{99}Mo-desorption properties of each Al_2O_3 specimen, (a) Day 1, (b) Day 2, (c) Day 3

Conclusions

To realize ^{99}Mo production by the activation method, we developed three types of Al_2O_3 specimens with different initial materials as Mo adsorbents and investigated ^{99}Mo-adsorption/^{99m}Tc-elution properties using neutron-irradiated MoO_3. Because of the ^{99}Mo-adsorption properties test in which the pH of the [^{99}Mo]Mo solution was changed, it was revealed that the Mo-adsorption capacity of Al_2O_3 increased when the acid concentration increased in the solution. The [^{99}Mo]molybdate species adsorbed on Al_2O_3 was assumed to be [^{99}Mo]MoO_4^{2-}, and it was concluded that the [^{99}Mo]Mo solution of pH 4 is suitable for adsorbing Mo on Al_2O_3. It was found the Mo-adsorption capacity and Mo-desorption properties of Al_2O_3 strongly depend on the specific surface of that. In addition, it is presumed a large amount of Mo-desorption causes an increase in the acid concentration of the ^{99m}Tc solution. The ^{99m}Tc-elution properties are considered to be influenced by the crystal structure of Al_2O_3 and it was particularly suggested the crystal structure of χ-Al_2O_3 was difficult to elute ^{99m}Tc. Therefore, it was concluded that improvement of specific surface and crystal structure is effective as factors for enhancing the properties of Al_2O_3. This result is useful for the development of Al_2O_3 with improved properties for application to ^{99}Mo/^{99m}Tc generators using (n, γ)^{99}Mo.

Acknowledgments

This study was conducted as a part of the joint use study at the Institute for Integrated Radiation and Nuclear Science, Kyoto University.

References

1. OECD-NEA (2011). The Supply of Medical Radioisotopes: An Assessment of Long-term Global Demand for Technetium-99m. Nuclear Development
2. OECD-NEA (2011). The Supply of Medical Radioisotopes: The Path to Reliability. Nuclear Development

3. OECD-NEA (2016). The Supply of Medical Radioisotopes: 2016 Medical Isotope Supply Review: ^{99}Mo/^{99m}Tc Market Demand and Production Capacity Projection 2016-2021. Nuclear Development NEA/SEN/HLGMR(2016)2

4. E. Bradley et al (2010). IAEA Activities to Support the Transition of Molybdenum-99 Production Away from the Use of Highly Enriched Uranium. RERTR 2010

5. H. Naik et al (2013). An alternative route for the preparation of the medical isotope ^{99}Mo from the ^{238}U(γ, f) and ^{100}Mo(γ, n) reactions. J Radioanal Nucl Chem. 295: 807-816

6. A. Gopalakrishna et al (2016). Preparation of ^{99}Mo from the ^{100}Mo(γ, n) reaction and chemical separation of ^{99m}Tc. J Radioanal Nucl Chem. 308: 431-438

7. M. Tanase et al (1997). A ^{99m}Tc Generator using a New Inorganic Polymer Adsorbent for (n, *γ*) ^{99}Mo. Appl Radiat Isot. 48: 607-611

8. S. Chattopadhyay et al (2017). Preparation of ^{99}Mo/^{99m}Tc generator based on cross-linked chitosan polymer using low-specific activity (n,*γ*)^{99}Mo. J Radioanal Nucl Chem. 313:647–653

9. I. Saptiama et al (2015). The Use of Sodium Hypochlorite Solution for (n,*γ*)^{99}Mo/^{99m}Tc Generator Based on Zirconium-Based Material (ZBM). Atom Indonesia. 41: 103-109

10. R. Chakravarty et al (2012). Preparation of clinical-scale ^{99}Mo/^{99m}Tc column generator using neutron activated low specific activity ^{99}Mo and nanocrystalline γ-Al_2O_3 as column matrix Nuclear Medicine and Biology. 39: 916-922

11. I.Saptiama, Y. V. Kaneti et al (2018). Template-Free Fabrication of Mesoporous Alumina Nanospheres Using Post-Synthesis Water-Ethanol Treatment of Monodispersed Aluminium Glycerate Nanospheres for Molybdenum Adsorption. Small. 14: 1800474

12. Kadarisman et al (2018). Synthesis of Nano-*α*-Al_2O_3 for ^{99}Mo Adsorbent. Atom Indonesia. 44: 17-21

13. M. Munir1 et al (2020). Development of mesoporous *γ*-alumina from aluminium foil waste for ^{99}Mo/^{99m}Tc generator. J Radioanal Nucl Chem. 326: 87–96

14. Y. Suzuki, T. Kitagawa et al (2018). Molybdenum Adsorption and Desorption Properties of Alumina with Different Surface Structures for ^{99}Mo/^{99m}Tc Generators. Trans Mat Res Soc Japan. 43: 75-80

15. W. H. Gitzen (1970). Alumina as a Ceramic Material. Wiley
16. Japan Radioisotope Association (2011). Isotope Pocket data Book, 11th edn. Tokyo
17. M. Kurosawa, K. Shimizu (1979). Estimation for Production of Molybdenum-99 Using (n, γ) Reaction. Journal of the Atomic Energy Society of Japan. 21: 505-509
18. G. L. Schmitt, D.J. Pietrzyk (1985). Liquid Chromatographic Separation of Inorganic Anions on an Alumina Column. Anal Cham. 57: 2247-2253
19. H. Jezlorowski, H. Knözinger (1979). Raman and Ultraviolet Spectroscopic Characterization of Molybdena on Alumina Catalysts. J Phys Chem. 83: 1166-1173
20. O. F. Oyerinde et al (2008). Solution structure of molybdic acid from Raman spectroscopy and DFT analysis. Inorganica Chimica Acta. 361: 1000-1007
21. K. Murata, S. Ikeda (1983). Studies on polynuclear molybdates in the aqueous solution by laser Raman spectroscopy. Spectrochimica Acrta. 39A: 787-794
22. G. M. S. El Shafei, N. A. Moussa, C. A. Philip (2000). Association of Molybdenum Ionic Species with Alumina Surface. Journal of Colloid and Interface Science. 228: 105-113
23. F.P.J.M.Kerkhof, J.A.Moulijn, R.Thomas (1979). Laser-Raman Spectroscopy of the Alumina-Supported Rhenium Oxide Metathesis Catalyst. Journal of catalysis. 56: 279-283
24. J. Steigman (1982). Chemistry of the Alumina Column. Int J Appl Radiat Isot. 33: 829-834

Supplementary information

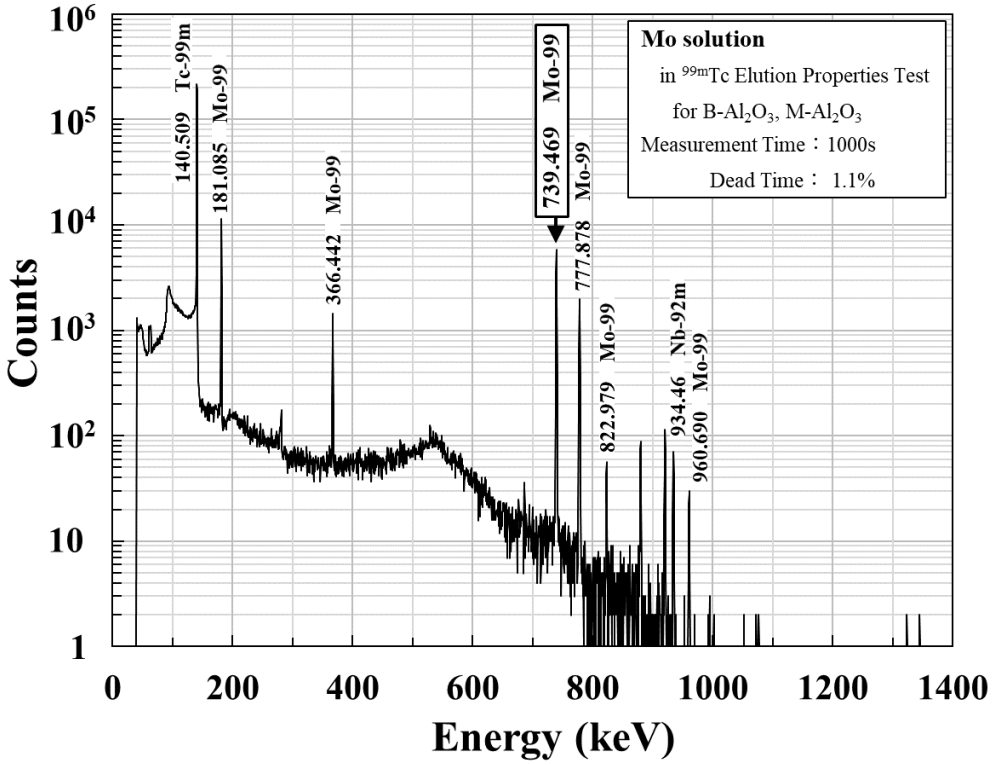

Fig. S1 The γ-ray spectrum of the [^{99}Mo]Mo solution and the peak (739.469 keV) used for the activity calculation of ^{99}Mo

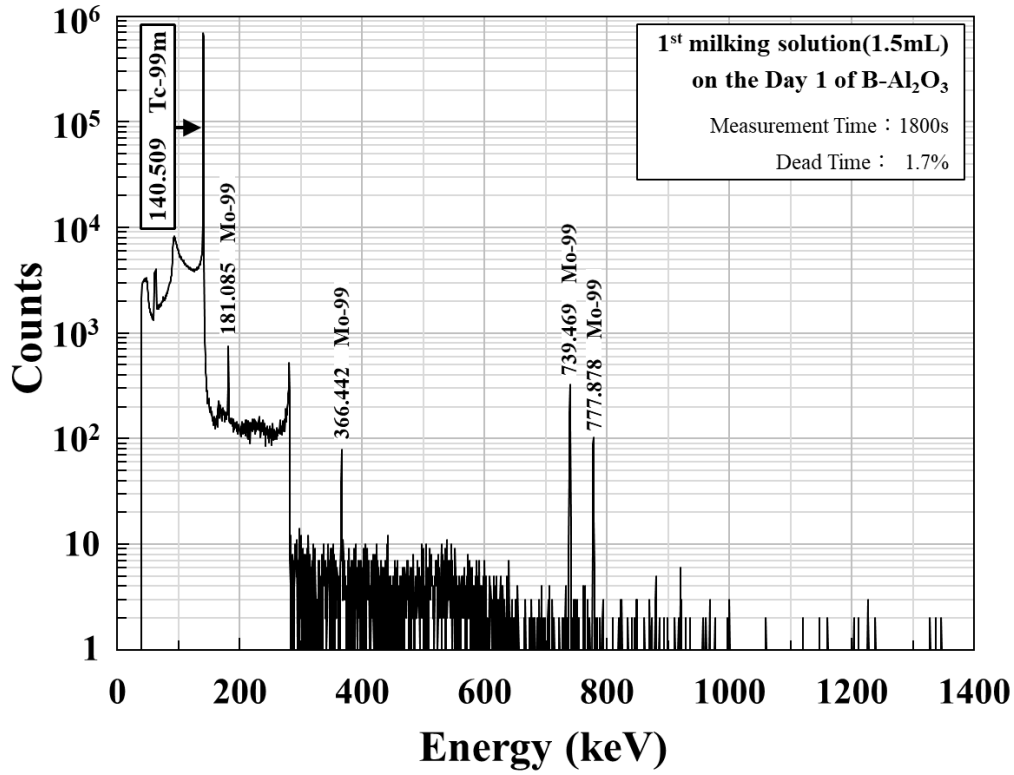

420

421 **Fig. S2** The *γ*-ray spectrum of the ^{99m}Tc solution and peak (140.509 keV) used for
422 activity calculation of ^{99m}Tc

423

424